ChemPubSoc Europe

DOI: 10.1002/chem.201302979

CHEMISTRY
A European Journal
Full Paper

Aptamers

Rational Design of a Redox-Labeled Chiral Target for an Enantioselective Aptamer-Based Electrochemical Binding Assay

Julie Moreau,[b] Lylian Challier,[b] Noémie Lalaoui,[b] François Mavré,[a] Vincent Noël,[b] Benoît Limoges,[a] Bernd Schöllhorn,*[a] and Claire Fave*[a, b]

Abstract: A series of redox-labeled L-tyrosinamide (L-Tym) derivatives was prepared and the nature of the functional group and the chain length of the spacer were systematically varied in a step-by-step affinity optimization process of the tracer for the L-Tym aptamer. The choice of the labeling position on L-Tym proved to be crucial for the molecular recognition event, which could be monitored by cyclic voltammetry and is based on the different diffusion rates of free and bound targets in solution. From this screening approach an efficient electroactive tracer emerged. Comparable dissociation constants K_d were obtained for the unlabeled and labeled targets in direct or competitive binding assays. The enantiomeric tracer was prepared and its enantioselective recognition by the corresponding *anti*-D-Tym aptamer was demonstrated. The access to both enantiomeric tracer molecules opens the door for the development of one-pot determination of the enantiomeric excess when using different labels with well-separated redox potentials for each enantiomer.

Introduction

Ligand binding assays take advantage of the selectivity of a biomolecular interaction (i.e., between a ligand and a receptor) to identify and quantify the presence of a molecule in a complex matrix.[1] They have found widespread applications in many fields such as clinical chemistry, drug development, food analysis, or environmental chemistry.[2–4] In some of these applications, the detection of chiral molecules might be of central importance. This is, for example, the case in the food industry for assaying food quality through the enantiomeric analysis of amino acids,[5] in the pharmaceutical industry by determination of enantiomeric excess, in forensic science for determining and quantifying illicit chiral substances,[3,6] or in environmental science for monitoring the fate of emerging chiral pollutants.[7] The development of rapid, simple, sensitive, and highly selective analytical methods for identifying and quantifying trace amounts of one enantiomer in a complex sample that contains its mirror image and many other unrelated molecules remains an important goal in analytical sciences. There are numerous types of ligand binding assays and, though techniques for direct monitoring of an interaction between a bioreceptor and an analyte have been increasingly proposed in recent years (e.g., surface plasmon resonance,[8] capillary electrophoresis,[9] or other related techniques), indirect methods associated with the quantitative detection of an extrinsic tracer (mostly a fluorescent label detected by an appropriate spectroscopic method) continue to be the focus of topical interest in the development of new and improved formats of ligand binding assays.[10–12] This has been well illustrated in the field of electrochemical biosensors, notably with the development of electronic DNA- or aptamer-based sensors that involve a redox-labeled oligonucleotide capture probe anchored onto an electrode surface.[13,14] Associated with these developments, different strategies of nucleic acid labeling by using diverse redox probes have been proposed.[15,16] In spite of the many practical advantages of electrochemical detection methods compared with optical ones, including high sensitivity, low-cost, robustness, field-portable capability, and ease of implementation, the principal inconvenience of DNA- or aptamer-based electrochemical sensors is the need to immobilize the redox-labeled capture probe on an electrode surface. An alternative to overcome this drawback, only scarcely reported so far, is to electrochemically monitor on a bare electrode the current response of a redox label engaged in a homogeneous ligand binding reaction. The few examples in the literature have been exclusively demonstrated for competitive homogeneous binding immunoassays. Only recently a homogeneous enantiospecific electrochemical ligand binding assay that relied on the combined use of an oligonucleotide–aptamer receptor with the electrochemical detection of a redox label has been proposed.[17] In this method, the principle of detection recalled

[a] *Dr. F. Mavré, Dr. B. Limoges, Prof. B. Schöllhorn, Dr. C. Fave*
Laboratoire d'Electrochimie Moléculaire, UMR 7591 CNRS
Université Paris Diderot, Sorbonne Paris Cité
15 rue Jean-Antoine de Baïf, 75205 Paris Cedex 13 (France)
Fax: (+33) 1-57-27-87-88
E-mail: bernd.schollhorn@univ-paris-diderot.fr
claire.fave@univ-paris-diderot.fr

[b] *Dr. J. Moreau, L. Challier, N. Lalaoui, Dr. V. Noël, Dr. C. Fave*
ITODYS, UMR 7086 CNRS
Université Paris Diderot, Sorbonne Paris Cité
15 rue Jean-Antoine de Baïf, 75205 Paris Cedex 13 (France)

Supporting information for this article is available on the WWW under http://dx.doi.org/10.1002/chem.201302979.

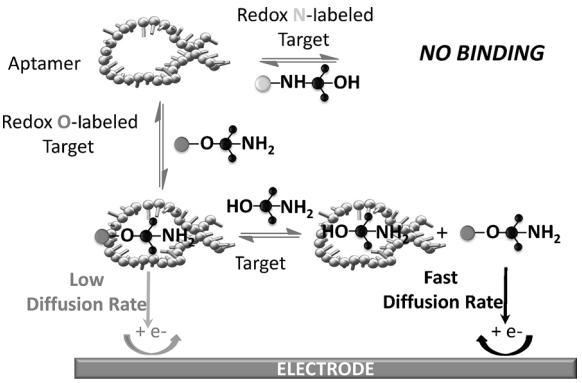

Figure 1. Principle of the aptamer-based competitive binding assay with electrochemical detection.

in Figure 1 basically depends on the difference of diffusion rates between the target molecule and the aptamer/target complex, and thus on the ability to detect the former more easily than the latter in homogeneous solution. The proof-of-concept of this electrochemical method was designed especially for the enantioselective detection of trace amounts of the small chiral model analyte L- or D-tyrosinamide (L- or D-Tym) by a single-stranded 49-mer D- or L-DNA receptor, respectively. On the basis of a homogeneous competitive binding assay strategy and of the electrochemical signal that resulted from the preferential detection of the free redox-labeled L-Tym, as little as 0.1% of the minor enantiomer in a non-racemic mixture could be achieved (equivalent to the determination of a 99.8% enantiomeric excess) in less than one minute.[17] Until now, the method has been validated for the homogeneous competitive binding assay of a single enantiomeric form of the analyte, but it is conceivable that the method could be extended to a simultaneous determination of the two enantiomeric forms in the same sample by employing two distinct redox probes, with each labeling one of the corresponding enantiomer analytes.

To move in this direction, a significant effort of synthesis and molecular engineering was required. Herein we describe the rational design and the systematic optimization of the tracer molecule properties.

For successful achievement of a homogeneous competitive binding assay, it is important that the labeling does not significantly affect the aptamer binding. Ideally, the redox-labeled analyte should have the same aptamer affinity binding as the unlabelled analyte and its size and solubility should not be significantly altered. The design of the labeled Tym derivative was thus guided by the following considerations. First, redox labels that showed fully reversible electron exchange with common electrodes in buffered aqueous solution were preferentially chosen because they are more amenable to a sensitive and reproducible detection. Clearly, the choice of chemically stable redox labels with an accessible electroactivity within the potential window of aqueous solutions is another important criterion. Because of their distinct standard potential (E^0) as well as of their high stability and fast reversible one-electron transfer process at an electrode, we selected as redox labels dicationic methylviologen (MV^{2+}) and ferrocene (Fc). Depending on the electron-donating or -withdrawing substituents, the standard potentials of methylviologen[18] (i.e., E^0 of the first reversible reduction of MV^{2+} into $MV^{\bullet+}$) and ferrocene (i.e., E^0 of the one-electron reversible oxidation of Fe^{II} to Fe^{III})[19] can be tuned from -0.5 to -0.7 V and from -0.2 to $+0.5$ V (versus Ag/AgCl), respectively. Another interesting property of methyviologen is its ability to efficiently electrocatalyze the reduction of dioxygen,[20] thus opening a way to amplify the sensitivity of detection of this redox label.

Because the exact structure of the Tym/aptamer complex has not yet been resolved, the effect of analyte labeling on the aptamer-binding recognition could not be anticipated. Therefore a screening approach based on a systematic change of the linking position as well as the spacer-chain length between the analyte and the redox label has been undertaken. Among various possible synthetic strategies, we favored the direct chemical labeling of the commercially available enantiomerically pure L-Tym. Such a straightforward approach aims to provide rapid and modular access to the corresponding redox-labeled molecules. Moreover, it could be easily extended to any other amino acid or analogue target using the same redox labels.

Although three likely labeling sites (Figure 2a, b, and c) can be easily identified in L-Tym, only positions a and b were investigated in the present work. In fact, modification of position c

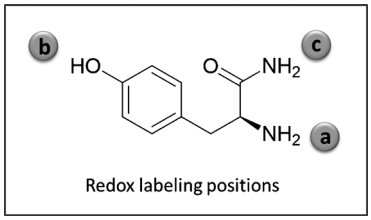

Figure 2. Redox labeling sites on L-Tym.

was previously shown by us[17] to completely impede the specific aptamer-binding recognition, thereby suggesting the amide function to be an indispensable motif for molecular recognition. Labeling through the amino group of L-Tym was the most natural since it was previously used in the systematic evolution of ligands by exponential enrichment (SELEX) to afford the final L-Tym aptamer (L-Tym was coupled to the SELEX solid phase through this function).[21] The primary amine was transformed into an amide linkage by means of a peptidic coupling or, alternatively, to a secondary amine link by means of reductive amination. Labeling of position b by means of a Mitsunobu coupling was used to afford ether derivatives, thereby suppressing the inherent electroactivity of Tym related to the oxidizable phenolic group.

Each redox-labeled L-Tym compound was then systematically tested for its enantiospecific recognition and affinity binding to the aptamer through a simple electrochemical titration assay, thereby providing immediate feedback on each prepared tracer as well as an accurate picture of the binding.

Once the best tracers were identified, their enantiomers were synthesized, thus opening a route to the development of an electrochemical competitive binding assay for the determination of the enantiomeric excess (*ee*) of L/D-Tym mixtures in one pot.

Results and Discussion

The rational step-by-step procedure that led to the design and synthesis of tyrosinamide derivatives is detailed below. The *O*-ferrocenyl L-Tym tracer L-**16** (Scheme 5 below) was previously shown to be well recognized by the aptamer.[17] Its dissociation constant ($K_d = (1.2 \pm 0.4)$ μM) was even found to be slightly better than that of the unlabeled L-Tym ($K_d = (3.8 \pm 0.7)$ μM), thus demonstrating that the labeling of L-Tym through the active hydroxyl group does not impede the aptamer-binding recognition.[17] This result also indicates that the hydrogen atom on the phenolic function does not significantly participate in the aptamer molecular recognition.

Amine labeling

Synthesis

Labeling of the L-Tym on the primary amine group afforded the water-soluble compounds L-**1** to L-**5** represented in Scheme 1. For the three dicationic derivatives L-**1** to L-**3**, the

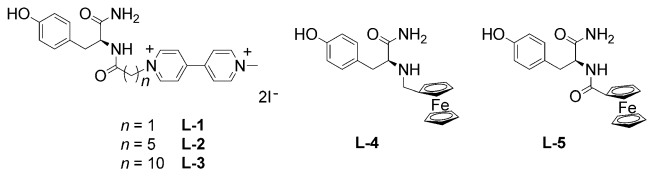

Scheme 1. N-Redox-labeled L-Tym targets.

redox-active methylviologen was separated from L-Tym by different chain lengths (one to ten methylene groups) in such a way as to anticipate the possible influence of positive charges and/or steric hindrance brought about by the pyridinium groups on molecular recognition. In the case of the ferrocenyl label, only the nature of the linking group was varied through the formation of a secondary amine (L-**4**) or a peptide link (L-**5**) (Scheme 1).

The synthesis of compounds L-**1** to L-**3** (Scheme 2) involved the formation of a bromide intermediate (L-**7** to L-**9**). The respective bromides were obtained in fairly good yields (50–85%) by the action of the corresponding bromocarboxylic acid derivative on L-Tym in the presence of the coupling reagent *N*,*N*,*N*′,*N*′-tetramethyl-*o*-(benzotriazol-1-yl)uranium tetrafluoroborate (TBTU). Substitution of the bromides with 1-methyl-4-pyridylpyridinium iodide in acetonitrile led to the formation of the corresponding MV^{2+}-labeled Tym L-**1** to L-**3**. The pure product could be easily isolated by precipitation in a mixture of acetonitrile and diethyl ether.

Compound L-**4** was obtained by the reaction of L-Tym with ferrocenyl carboxaldehyde and subsequent reduction of the intermediate imine with sodium borohydride to afford the secondary amine L-**4** in 40% yield (Scheme 3). Compound L-**6** was prepared in a similar way to assess the influence of the steric hindrance on the amino position on the binding affinity to the aptamer. Derivative L-**5** was obtained in 60% yield by means of peptide coupling that involved the ferrocene carboxylic acid and both diisopropylethylamine (DIPEA) and TBTU.

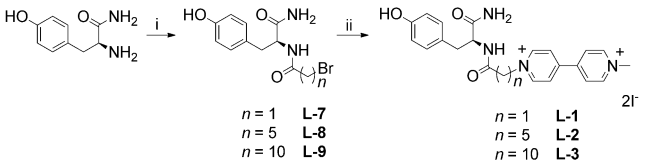

Scheme 2. Synthesis of viologen L-Tym derivatives L-**1** to L-**3**: i) Br-$(CH_2)_nCO_2H$, TBTU, DIPEA, EtOAc, 50–85%; ii) *N*-methyl-4-pyridylpyridinium iodide salt, CH_3CN, 80 °C, 48 h, 36–95%.

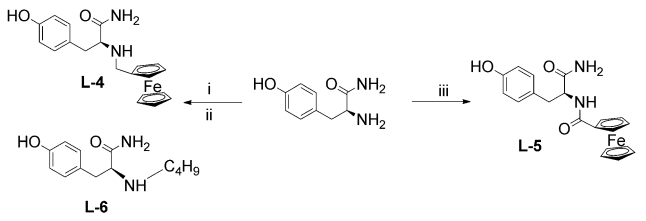

Scheme 3. Synthesis of ferrocenyl-labeled L-Tym derivatives L-**4** to L-**6**: i) FcCHO or C_3H_7CHO, NEt_3, MeOH; ii) $NaBH_4$, 4 °C, 40–85%; iii) FcCOOH, TBTU, DIPEA, EtOAc, 60%.

Electrochemical properties

Electrochemical experiments were carried out by using cyclic voltammetry (CV) in a deaerated tris(hydroxymethyl)aminomethane (Tris) buffer (pH 7.4) and using carbon-based screen-printed electrodes. For compounds L-**1** to L-**3**, two monoelectronic reversible waves were systematically observed in the cyclic voltammograms (Figure 3A, Table 1), which were characteristic of the two successive one-electron reductions of the dication MV^{2+} to a monocation $MV^{\bullet+}$ and then to a neutral com-

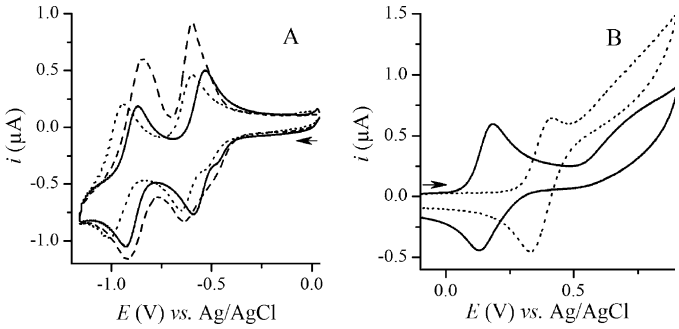

Figure 3. A) Cyclic voltammograms of L-**1** (solid line), L-**2** (dotted), and L-**3** (dashed). B) Cyclic voltammograms of L-**4** (dotted) and L-**5** (solid). The experiments were achieved in L-Tym (50 μM) derivative in Tris buffer solution (pH 7, $v = 0.1\ V\,s^{-1}$).

Table 1. Redox potentials (versus Ag/AgCl) and dissociation constants of the redox-labeled Tym derivatives.[a]

Compound	L-**1**	L-**2**	L-**3**	L-**4**	L-**5**	L-**15**	L-**16**	L-**17**
E_1^0 [V]	−0.55	−0.62	−0.62	+0.15	+0.37	−0.57	+0.17	+0.02
E_2^0 [V]	−0.90	−0.97	−0.88	–	–	−0.89	–	–
ΔEp_1 [mV]	52	56	43	80	58	60	62	64
ΔEp_2 [mV]	60	65	82	–	–	68	–	–
K_d [μM]	n.r.	n.r.	n.r.	n.r.	n.r.	0.6	1.2	n.r.

[a] ΔEp = peak potential difference. n.r. = no recognition.

pound at approximately −0.6 and −1.0 V (versus Ag/AgCl), respectively.

The increasing alkyl chain length between the viologen entity and L-Tym induces only weak anodic shifts of the standard potentials for both reversible waves (Figure 3A, Table 1). Cyclic voltammograms of the ferrocene-labeled compounds L-**4** and L-**5** (Figure 3B, Table 1) show both a single monoelectronic reversible oxidation wave located at +0.15 and +0.37 V (versus Ag/AgCl), respectively, followed by an ill-defined irreversible anodic wave at approximately +0.7 V. The standard potential difference of the ferrocenyl groups is in agreement with the electron-withdrawing effect of the differently substituted cyclopentadienyl groups. The carbonyl substituent in L-**5** is a stronger electron-withdrawing group than the methylene substituent in L-**4**, thereby shifting the E^0 of ferrocene to a higher value. The ill-defined irreversible anodic peak observed for each molecule at approximately +0.7 V is typical of the irreversible oxidation of the phenol group (see the cyclic voltammogram of L-Tym in Figure S1 of the Supporting Information).[22]

Aptamer-binding recognition tests

To evaluate whether the redox-labeled L-Tym derivatives were recognized by the 49-mer *anti*-L-Tym, binding recognition tests were carried out. For such purposes, the magnitude of the anodic or cathodic CV peak current of a redox-labeled L-Tym compound (5 μM in solution) was monitored as a function of increasing aptamer concentration. The CV peak current of the redox label was expected to decrease when the redox-labeled target was recognized by the aptamer. Unfortunately, for all tracer compounds L-**1** to L-**5**, a stable signal was observed, even for large excess amounts of aptamer, thus indicating a complete loss of the specific binding recognition. This result suggests the crucial role of the primary amino group in the recognition process. To confirm this hypothesis and also to verify if it might not be the result of a steric effect on the molecular recognition owing to the presence of the bulky ferrocenyl group, compound L-**6** was tested. To suitably electrochemically detect L-**6** in the presence of D-Apt_{49}, we used the redox-mediated catalytic oxidation of the phenolic group of L-Tym (this was achieved by adding a minute amount of the redox mediator $[Os^{II}(bpy)_3]^{2+}$ (bpy = 2,2′-bipyridyl) to the binding solution as previously described).[17] However, as shown in Figure 4, no significant current response decrease could be observed in contrast to the well-defined asymptotic signal decrease obtained with L-Tym, thus demonstrating the absence of L-**6** recognition by the aptamer and confirming the critical role of the free amino group in the recognition of labeled derivatives by the aptamer (the small signal diminution observed with L-**6** in Figure 4 is attributed to a nonspecific response decrease since it is similar to the one obtained with L-Tym in the presence of an increasing amount of a 49-mer random DNA sequence).[17]

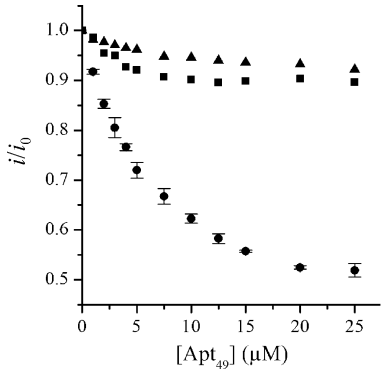

Figure 4. Normalized catalytic peak current as a function of aptamer concentration for the following ligand/receptor couples: (●) L-Tym/D-Apt_{49}, (■) L-**6**/D-Apt_{49}, and (▲) L-Tym/49-mer scrambled oligonucleotide. Each data point represents the average of three measurements. The indicated error bars are standard deviations. (Data are extracted from CV of Tris buffer (5 mM, pH 7) solutions containing $[Os(bpy)_3]^{2+}$ (1 μM), L-Tym, or L-**6** (5 μM), NaCl (50 mM), $MgCl_2$ (10 mM), and increasing concentrations of Apt_{49}.)

Phenol labeling

Synthesis of the L-Tym tracers

To corroborate our previous results obtained with L-**16**,[17] labeling of the L-Tym phenolic position (Figure 2) was explored with different redox probes, leaving the primary amino group unchanged. The viologen-labeled derivative L-**15** was obtained according to a five-step synthesis. The strongly nucleophilic amino group first had to be protected. The phenolic group of the *N-tert*-butoxycarbonyl (Boc)-protected derivative L-**11** was then treated with 1-bromo-3-chloropropane in the presence of potassium carbonate to lead to compound L-**12** in 65% yield. Substitution of chloride L-**12** by 4,4′-bipyridine followed by *N*-methylation afforded the viologen derivative L-**14** as an iodide salt. Removal of the Boc protecting group was obtained in a mixture of trifluoroacetic acid and dichloromethane, thus leading to L-**15** as a trifluoroacetate salt (Scheme 4).

The analogue ferrocenyl derivative L-**16** (Scheme 5) was obtained by means of a Mitsunobu reaction of L-Tym and ferrocene methanol using the conditions of a previously published procedure.[23] Because of its low oxidation potential (close to 0 V versus Ag/AgCl), pentamethylferrocene is an interesting alternative redox label as well. The synthesis of pentamethylferrocene methanol was performed according to an adaptation of a previously described protocol.[24] Its coupling to L-Tym was performed under the same conditions as described above.

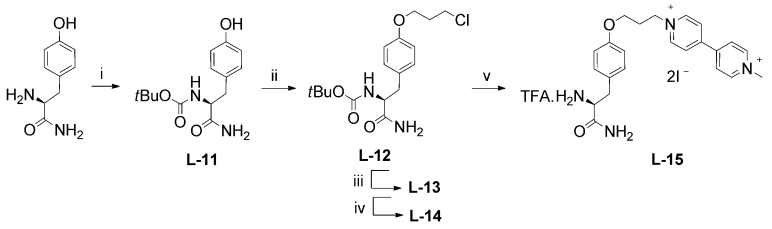

Scheme 4. Synthesis of the viologen L-Tym derivative L-**15**: i) $(Boc)_2O$, dioxane, NaOH, 58%; ii) $Br(CH_2)_3Cl$, K_2CO_3, DMF, 65%; iii) 4,4′-bipyridine, CH_3CN, KI, 58%; iv) MeI, CH_3CN, 25%; v) TFA/CH_2Cl_2 (50:50), 95%. TFA = trifluoroacetic acid.

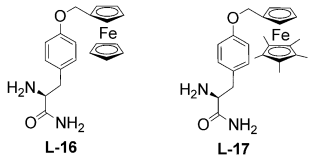

Scheme 5. Ferrocenyl-labeled derivatives L-**16** and L-**17**.

Compound L-**17** was obtained in a modest yield (13%), probably due to its weak electrophilicity and fair solubility.

Electrochemical properties

CV of a deaerated solution of L-**15** shows (Table 1), as expected, the presence of two reversible waves at −0.57 and −0.89 V (versus Ag/AgCl), which are characteristic of the presence of viologen on the molecule (data not shown). These E^0 values were not significantly different from those previously obtained for L-**1** to L-**3**. Oxidation of the ferrocenyl- and pentamethylferrocenyl-labeled compounds L-**16** and L-**17** occurred at +0.17 and +0.02 V, respectively (Figure 5, Table 1). These results are

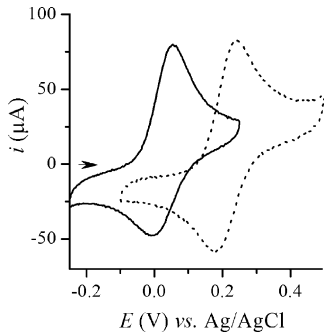

Figure 5. Cyclic voltammograms of L-**16** (dotted line) and L-**17** (solid) at 5 μM in Tris buffer (pH 7, $v = 0.05\ V\,s^{-1}$).

consistent with the oxidation potentials $E^0 = +0.25$ and −0.05 V obtained for the corresponding precursor compounds, that is, ferrocene methanol and pentamethylferrocene methanol. The lower E^0 value of the latter results from the strong electron-donating effect of the pentamethylcyclopentadienyl ligand. The electrochemical properties of compounds D-**15** and D-**16** were the same as their enantiomeric forms L-**15** and L-**16** (data not shown).

Aptamer-binding recognition tests

In contrast to compound L-**16**, for which a good affinity binding to D-Apt_{49} was obtained (K_d = 1.2 μM),[17] the aptamer binding test with L-**17** was unsuccessful, thus suggesting complete loss of recognition (Table 1). Presently there is no explanation for this result, but we might postulate that the high hydrophobicity of the pentamethylferrocenyl label as well as its bulky size should interfere in the recognition process. The viologen derivative L-**15** was also tested for its binding to the D-Apt_{49}, but instead of CV we preferred to use square-wave voltammetry (SWV). This technique has the advantage of being more sensitive than CV and providing better-defined and more reproducible current responses when working with micromolar concentrations of MV^{2+}. The magnitude of the SWV peak currents of 2 μM L-**15** (the second reduction peak current that corresponded to the $MV^{\bullet+}/MV^0$ couple was used as the analytical response) was monitored as a function of the aptamer concentration. The decrease in the two peaks upon addition of D-Apt_{49} clearly shows that the labeled target L-**15** is well recognized by the aptamer. From the data fitting, a value of $K_d = (0.6 \pm 0.2)$ μM was inferred. This value is twice as low as the analogous ferrocenyl-labeled compound L-**16** and approximately six times better than the unlabeled L-Tym (3.8 μM).

These results show that labeling of L-Tym through the phenolic position, even if not without its limitations, is the most suitable way for preserving the specific binding to the aptamer.

With all these results in hand, we next performed an electrochemical competitive binding assay to confirm the K_d value obtained for L-**15** with the previous approach. In these experiments, the competitive assay was achieved from a starting solution that contained 5 μM L-**16** and 10 μM D-Apt_{49}, and an increasing amount of L-**15** (Figure 6A) or L-**2** (Figure 6B) analytes.

The decrease in the anodic and cathodic peak currents upon the addition of D-Apt_{49} was anticipated due to the previously well-established enantiospecific recognition of L-**16** by the aptamers (black to gray in Figure 6A and B). Adding increasing amounts of L-**15** to this solution gave a steady increase in the reversible voltammetric peak currents of ferrocene (Figure 6A), whereas an increasing addition of L-**2** did not change anything (Figure 6B). The resulting competitive calibration plots are shown in Figure 7C. These results definitely demonstrate the absence of recognition between L-**2** and D-Apt_{49}. From the fit of the experimental data obtained with L-**15** to the theoretical equation used for a competitive binding,[17] a value of $K_d = (0.4 \pm 0.1)$ μM was inferred, which is in very good agreement with the value determined directly ($K_d = (0.6 \pm 0.2)$ μM) from the titration plot in Figure 6B.

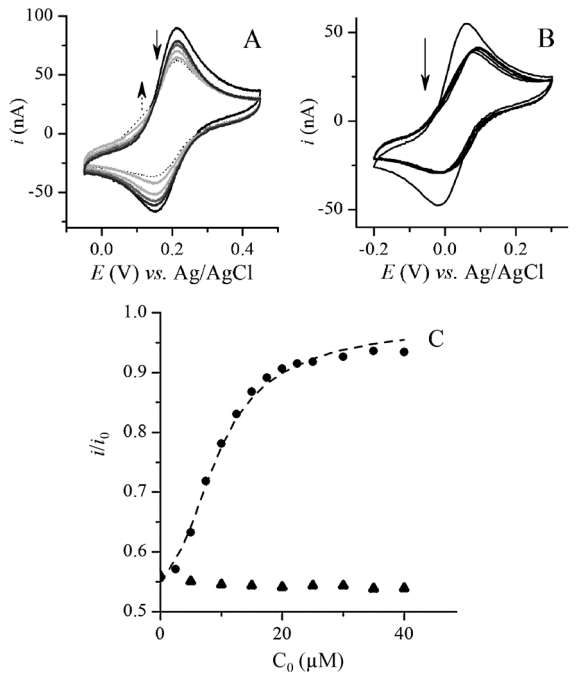

Figure 6. A) Cyclic voltammograms ($v = 0.05\ V\,s^{-1}$) in Tris buffer (5 mM, pH 7.4, 50 mM NaCl, 10 mM Mg^{2+}) of L-**16** (5 μM; black curve), L-**16** (5 μM), and D-Apt_{49} (10 μM) (-----) and an increasing amount of L-**15**: 5, 10, 15, 40 μM (gray). B) Same as in (A) but for an increasing amount of L-**2**. C) Competitive binding curves for L-**15** (●) and L-**2** (▲). Dashed line: Fit to the theoretical equation of a competitive binding.

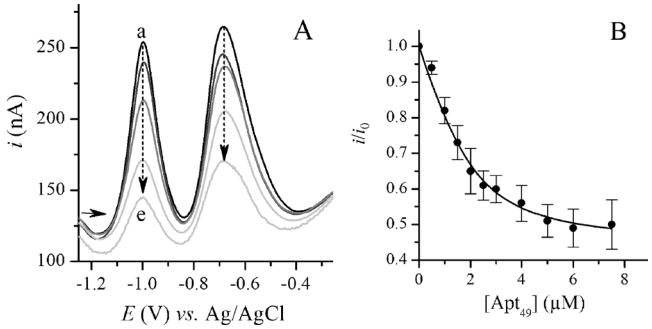

Figure 7. A) Square-wave voltammograms ($f = 25$ Hz, $\Delta E = 20$ mV, $E_{step} = 5$ mV) of L-**15** (2 μM) in Tris buffer (5 mM, pH 7.4) solution containing NaCl (50 mM), Mg^{2+} (10 mM), and a) 0, b) 1, c) 2, d) 3, and e) 7.5 μM D-Apt_{49}. B) Normalized peak (at −1.0 V) current response as a function of aptamer concentration. Each data point is the average of three measurements. Error bars are standard deviations.

Synthesis of the D-Tym tracers

Given the proper binding recognition of L-**15** and L-**16** by D-Apt_{49}, the mirror image tracers D-**15** and D-**16** were prepared. The synthesis of the viologen-labeled D-Tym D-**15** was obtained from the commercially available starting compound D-tyrosine. Measurement of the optical rotation of the Boc-protected derivative D-**11** gave a value of $[\alpha]_{25}^{D} = -20.1\,^{\circ}\,mL\,cm^{-3}\,g^{-1}$ (1 $g\,mL^{-1}$, MeOH), which is in good agreement with its enantiomer L-**11** $[\alpha]_{25}^{D} = +22.5\,^{\circ}\,mL\,cm^{-3}\,g$ (1 $g\,mL^{-1}$, MeOH). Compound D-**15** was obtained from D-**11** with a global yield of 54% by following the same procedure as described for the synthesis of L-**15**.

The synthesis of the ferrocenyl tracer D-**16** was achieved by nucleophilic substitution of a ferrocenyl trimethylammonium salt with the commercial D-Tym hydrochloride in DMSO in the presence of a 10% aqueous NaOH solution (2 equiv).[25] DMSO was used to enhance the base-catalyzed reactions. A similar procedure had been previously reported by Solar and Schumaker for the selective *O*-alkylation of tyrosine derivatives.[26] After 2 h of heating at 80 °C, only 20% conversion was revealed by ^{1}H NMR spectroscopy, and longer reaction times resulted in complete decomposition of the product. Liquid chromatography of the crude reaction mixture afforded D-**16** in 20% yield. The specific rotation values reported in Table 2 confirm the presence of the enantiomeric tracer molecules L-/D-**15** and L-/D-**16**.

Table 2. Specific rotation of the redox-labeled Tym compounds in methanol.

Compound	$[\alpha]_{25}^{D}$ [° mL cm^{-3} g^{-1})]	*C* [g mL^{-1}]
L-**15**	+1.84	0.40
D-**15**	−3.56	0.34
L-**16**	+2.92	0.33
D-**16**	−3.10	0.31

The aptamer-binding recognition tests were next performed for each ferrocene-labeled enantiomer of L-Tym. As expected, D-**16** was not recognized by D-Apt49 but rather only by the mirror image aptamer L-Apt49 (Figure 8). A K_d value of 1.4 μM was obtained for the latter, which is nearly the same value as for the L-enantiomeric ligand/receptor couple.

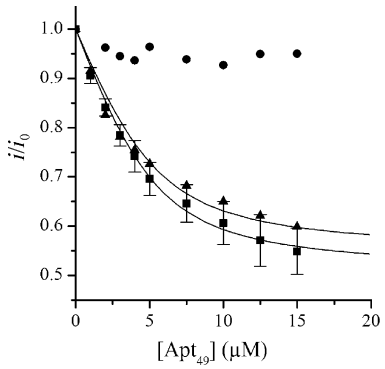

Figure 8. Normalized catalytic peak current as a function of aptamer concentration for the ligand/receptor couples: D-**16**/D-Apt_{49} (●), D-**16**/L-Apt_{49} (▲), L-**16**/D-Apt_{49} (■).

Conclusion

A series of redox-labeled L-tyrosinamide derivatives was prepared. The nature of the functional group and the chain length of the spacer were systematically varied in a step-by-

step optimization process of the tracer for its *anti*-L-Tym aptamer. The homogeneous binding recognition events were efficiently monitored by cyclic voltammetry by taking advantage of the difference in diffusion rates between the free and bound targets in solution. The results demonstrate the crucial role of the primary amino group of tyrosinamide in the aptamer binding recognition process. In contrast, alkylation of the phenolic group did not significantly influence the affinity properties. Comparable dissociation constants K_d were finally obtained for the unlabeled and labeled targets in a direct or competitive binding assay. Furthermore, the redox-labeled enantiomeric form of L-Tym was prepared and its enantioselective recognition by the corresponding mirror image aptamer was demonstrated. The possibility afforded by the labeling of the two enantiomeric forms of the tyrosinamide target by two distinct redox labels (i.e., with well-separated redox potentials) opens the opportunity to develop an enantiomeric competitive binding assay for the determination of the enantiomeric excess in a single analysis. Beyond this particular example of an enantiospecific competitive binding assay, the present electrochemical detection method is of more general interest since it can be relatively easily extended to a wide range of other small target molecules able to specifically bind to an aptamer. Moreover, combined with multiple redox labeling, it would be promising for the development of a multiple analysis in the same sample.

Acknowledgements

This work was supported by Agence Nationale pour la Recherche (ANR project ECSTASE). Noémie Lalaoui thanks the ITODYS Laboratory for a grant. We thank David Clainquart (Chemistry Department, Université Paris Diderot) for his help with GC-MS measurements.

Keywords: aptamers · chirality · electrochemistry · enantioselectivity · redox labeling

[1] M. N. Khan, J. W. Findlay, *Ligand-Binding Assays: Development, Validation and Implementation in the Drug Development Arena*, Wiley, Hoboken, **2009**.
[2] V. García-Cañas, C. Simo, M. Herreo, E. Ibanez, A. Cifuentes, *Anal. Chem.* **2012**, *84*, 10150 – 10159.
[3] J. T. Liu, R. H. Liu, *J. Biochem. Biophys. Methods* **2002**, *54*, 115 – 146.
[4] E. Eljarrat, P. Guerra, D. Barcelo, *TrAC Trends Anal. Chem.* **2008**, *27*, 847 – 861.
[5] M. Herrero, C. Simo, V. Garcia-Canas, S. Fanali, A. Cifuentes, *Electrophoresis* **2010**, *31*, 2106 – 2114.
[6] F. P. Smith in *Handbook of Forensic Drug Analysis* (Ed.: J. A. Siegel), Elsevier, Amsterdam (The Netherlands), **2005**.
[7] J. R. Kucklick, P. A. Helm, *Anal. Bioanal. Chem.* **2006**, *386*, 819 – 836.
[8] J. Homola, *Anal. Bioanal. Chem.* **2003**, *377*, 528 – 539.
[9] V. Poinsot, M. A. Carpéné, J. Bouajila, P. Gavard, B. Feurer, F. Couderc, *Electrophoresis* **2012**, *33*, 14 – 35.
[10] D. S. Smith, S. A. Eremin, *Anal. Bioanal. Chem.* **2008**, *391*, 1499 – 1507.
[11] J. Liu, Z. Cao, Y. Lu, *Chem. Rev.* **2009**, *109*, 1948 – 1998.
[12] H. Zhang, F. Li, B. Dever, X.-F. Li„ X. C. Le, *Chem. Rev.* **2013**, *113*, 2812 – 2841.
[13] A. A. Lubin, K. W. Plaxco, *Acc. Chem. Res.* **2010**, *43*, 496 – 505.
[14] J.-O. Lee, H.-M. So, E.-K. Jeon, H. Chang, K. Won, Y. H. Kim, *Anal. Bioanal. Chem.* **2008**, *390*, 1023 – 1032.
[15] M. Hocek, M. Fojta, *Chem. Soc. Rev.* **2011**, *40*, 5802 – 5814.
[16] J. Moreau, N. Dendane, B. Schöllhorn, N. Spinelli, C. Fave, E. Defrancq, *Bioorg. Med. Chem. Lett.* **2013**, *23*, 955 – 958.
[17] L. Challier, F. Mavré, J. Moreau, C. Fave, B. Schöllhorn, D. Marchal, E. Peyrin, V. Noël, B. Limoges, *Anal. Chem.* **2012**, *84*, 5415 – 5420.
[18] C. P. Andrieux, P. Hapiot, J. M. Savéant, *J. Electroanal. Chem.* **1985**, *189*, 121 – 133.
[19] S. Lu, V. V. Strelets, M. F. Ryan, W. J. Pietro, A. B. P. Lever, *Inorg. Chem.* **1996**, *35*, 1013 – 1023.
[20] J. M. Savéant, *Chem. Rev.* **2008**, *108*, 2348 – 2378.
[21] E. Vianini, M. Palumbo, B. Gatto, *Bioorg. Med. Chem.* **2001**, *9*, 2543 – 2548.
[22] C. Costentin, C. Louault, M. Robert, J. M. Savéant, *Proc. Natl. Acad. Sci. USA* **2009**, *106*, 18143 – 18148.
[23] C. Baldoli, L. Falciola, E. Licandro, S. Maiorana, P. Mussini, P. Ramani, C. Rigamonti, G. Zinzalla, *J. Organomet. Chem.* **2004**, *689*, 4791 – 4802.
[24] F. M. Geisler, G. Helmchen, *Synthesis* **2006**, *13*, 2201 – 2205.
[25] S. L. Solar, R. R. Schumaker, *J. Org. Chem.* **1966**, *31*, 1996 – 1997.
[26] G. Tang, X. Tang, M. Wang, L. Luo, M. Gan, Z. Huang, *J. Labelled Compd. Radiopharm.* **2003**, *46*, 661 – 668.

Received: July 29, 2013
Published online on February 12, 2014